Title

When and how did the terrestrial mid-Permian mass extinction occur? Evidence from the tetrapod record of the Karoo Basin, South Africa

Journal

Proceedings of the Royal Society B, 282(1811)

ISSN

0962-8452

Authors

Day, Michael O

Ramezani, Jahandar

Bowring, Samuel A

et al.

Publication Date

2015-07-22

DOI

10.1098/rspb.2015.0834

Peer reviewed

PROCEEDINGS B

rspb.royalsocietypublishing.org

Research

Cite this article: Day MO, Ramezani J, Bowring SA, Sadler PM, Erwin DH, Abdala F, Rubidge BS. 2015 When and how did the terrestrial mid-Permian mass extinction occur? Evidence from the tetrapod record of the Karoo Basin, South Africa. *Proc. R. Soc. B* **282**: 20150834.
http://dx.doi.org/10.1098/rspb.2015.0834

Received: 11 April 2015
Accepted: 5 June 2015

Subject Areas:
palaeontology

Keywords:
biostratigraphy, Permian, Karoo, tetrapod extinction, U–Pb geochronology, Guadalupian

Author for correspondence:
Michael O. Day
e-mail: michael.day@wits.ac.za

Electronic supplementary material is available at http://dx.doi.org/10.1098/rspb.2015.0834 or via http://rspb.royalsocietypublishing.org.

THE ROYAL SOCIETY PUBLISHING

When and how did the terrestrial mid-Permian mass extinction occur? Evidence from the tetrapod record of the Karoo Basin, South Africa

Michael O. Day[1], Jahandar Ramezani[2], Samuel A. Bowring[2], Peter M. Sadler[3], Douglas H. Erwin[4], Fernando Abdala[1] and Bruce S. Rubidge[1]

[1]Evolutionary Studies Institute, School of Geosciences, University of the Witwatersrand, Private Bag 3, Johannesburg 2050, South Africa
[2]Department of Earth, Atmospheric and Planetary Sciences, Massachusetts Institute of Technology, Cambridge, MA 02139, USA
[3]Department of Earth Sciences, University of California, Riverside, CA 92521, USA
[4]Department of Paleobiology, National Museum of Natural History, Washington, DC 20013-7012, USA

A mid-Permian (Guadalupian epoch) extinction event at approximately 260 Ma has been mooted for two decades. This is based primarily on invertebrate biostratigraphy of Guadalupian–Lopingian marine carbonate platforms in southern China, which are temporally constrained by correlation to the associated Emeishan Large Igneous Province (LIP). Despite attempts to identify a similar biodiversity crisis in the terrestrial realm, the low resolution of mid-Permian tetrapod biostratigraphy and a lack of robust geochronological constraints have until now hampered both the correlation and quantification of terrestrial extinctions. Here we present an extensive compilation of tetrapod-stratigraphic data analysed by the constrained optimization (CONOP) algorithm that reveals a significant extinction event among tetrapods within the lower Beaufort Group of the Karoo Basin, South Africa, in the latest Capitanian. Our fossil dataset reveals a 74–80% loss of generic richness between the upper *Tapinocephalus* Assemblage Zone (AZ) and the mid-*Pristerognathus* AZ that is temporally constrained by a U–Pb zircon date (CA-TIMS method) of 260.259 ± 0.081 Ma from a tuff near the top of the *Tapinocephalus* AZ. This strengthens the biochronology of the Permian Beaufort Group and supports the existence of a mid-Permian mass extinction event on land near the end of the Guadalupian. Our results permit a temporal association between the extinction of dinocephalian therapsids and the LIP volcanism at Emeishan, as well as the marine end-Guadalupian extinctions.

1. Introduction

An 'end-Guadalupian' extinction, distinct from that at the end of the Permian, was first recognized in the marine realm in the 1990s [1,2]. Shortly afterwards it was calculated to be one of the most catastrophic extinction events of the Phanerozoic [3] and since then a considerable body of work has attempted to explore it, focusing on carbonate platforms of southern China and Japan [4–9]. Some recent studies have identified extinction horizons preceding the Guadalupian–Lopingian boundary (GLB) by several conodont zones [7,8] and therefore conclude that the mid-Permian marine extinctions constitute an intra-Capitanian event. This older age appears to be corroborated by new data from high latitude boreal sequences from Spitzbergen [10]. However, extinction horizons have been identified for a number of Guadalupian invertebrate taxa at various biostratigraphic levels between the late Capitanian *Jinogondolella prexuanhanensis/xuanhanensis* Conodont Zone and the earliest Lopingian *Clarkina postbitteri postbitteri* Conodont Zone [6,7]. The ages of the marine extinctions therefore remain unclear but mostly appear to occur

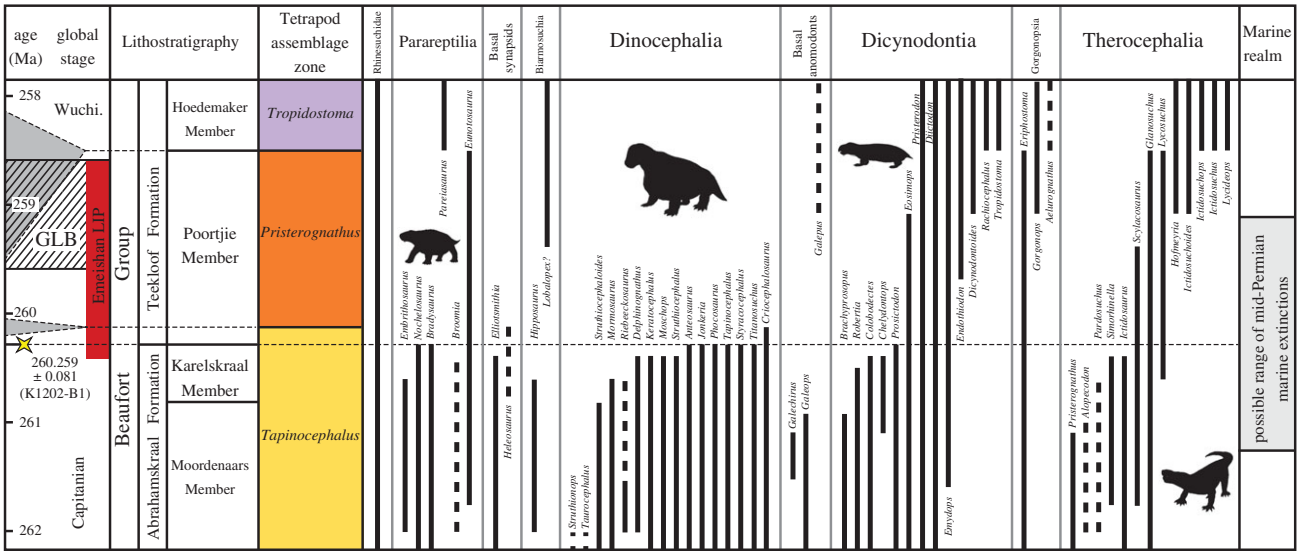

Figure 1. Minimum stratigraphic ranges of tetrapod genera across the mid-late Permian boundary in the Karoo Basin. The shaded triangles on the left indicate uncertainty surrounding the age of biozone boundaries (electronic supplementary material, Methods). Genera from the *Tropidostoma* AZ presented here are only those believed to occur in the lowest part of that AZ. The age of the marine extinctions is taken from the literature cited in the text. Star, dated horizon presented here; Wuchi., Wuchiapingian. (Online version in colour.)

before the GLB, for which the current age estimate of 259.1 ± 0.5 Ma is derived from links to the termination of volcanism in the Emeishan Large Igneous Province (LIP) [11,12].

In the terrestrial realm, at least one extinction event among plant species has been identified in the Capitanian Upper Shihhotse Formation of Northern China, suggesting the loss of at least 56% of plant species within this stage [13]. Unfortunately, the age estimates for this sequence rely on palaeomagnetism and missing data within the stratigraphic profile has led to high uncertainty in their correlation with the marine timescale. Among tetrapods, diverse mid-Permian assemblages characterized by dinocephalian therapsids are known around the world but primarily from Russia and South Africa [14]. Younger therapsid faunas of late Permian age do not contain dinocephalians and this has led to the proposal of a global 'dinocephalian extinction event' [15], which is best recorded in the Beaufort Group of South Africa's Main Karoo Basin, where the abundance of fossil tetrapods has enabled its subdivision into vertebrate assemblage zones [16]. The extinction of dinocephalian therapsids occurred in the uppermost *Tapinocephalus* Assemblage Zone (AZ), which is most widely exposed in the southwest of the basin, where it is situated stratigraphically close to the boundary of the Abrahamskraal and overlying Teekloof formations (figure 1). In the past, stratigraphic collecting within the lowest Beaufort strata was limited and most fossil specimens collected from there have imprecise provenance data. Consequently, the stratigraphic ranges of most genera from the *Tapinocephalus* AZ have been attributed only to that biozone rather than to a discrete stratigraphic interval [16]. Although the disappearance of the diverse dinocephalian fauna had been recognized [17,18], such broad assignments and poor correlation have led to the misinterpretation of Permian tetrapod diversity changes and the extrapolation of an artificial extinction 'horizon' at the top of the *Tapinocephalus* AZ [19].

Limited chemostratigraphic data have been used to suggest a correlation between the extinction of dinocephalians in South Africa and the end-Guadalupian marine extinctions [19]. However, carbon isotope correlations for the Capitanian may be dubious [15,20] and most recent studies have instead accepted that the dinocephalian extinction is most probably constrained to the Wordian on the basis of allegedly stronger magnetostratigraphic correlations, thus predating the Capitanian extinctions [8,13,15]. This relies on the restriction of Russian dinocephalian faunas to strata below the Illawarra geomagnetic reversal [21], which has been tentatively assigned to the latest Wordian or perhaps even earlier [22–24]. Conversely, the presence of normal polarity in the lower Abrahamskraal Formation suggests the dinocephalian extinctions in South Africa postdate the Illawarra reversal [24]. Although it is possible that the last occurrences of dinocephalians in Eastern Europe and South Africa were diachronous, biostratigraphic correlations support the equivalence of the *Tapinocephalus* AZ and youngest Russian dinocephalian assemblage (Isheevo) [14,15,25], making the existence of a large temporal discrepancy unlikely. The overlying *Pristerognathus* AZ, however, has not been directly correlated with an Eastern European equivalent. In most cases, the *Pristerognathus* AZ is either ignored [14] or is placed rather arbitrarily at an equivalent horizon to the *Deltavjatia vjatkensis* AZ, probably because of their status as the first 'post-dinocephalian' assemblages (e.g. [25]). Kurkin [26] noticed that the distribution of dicynodont therapsids suggests the *Deltavjatia* AZ may have closer affinities to the late Permian South African *Tropidostoma* AZ (figure 1), which would leave the *Pristerognathus* AZ in limbo between the *Ulemosaurus* and *Deltavjatia* AZs. The correlation of the *Pristerognathus* AZ with Eastern Europe remains uncertain but Russian authors consider the dinocephalian extinction in Russia to fall close to the end of the Guadalupian [25,26].

Recent U–Pb CA-TIMS geochronology from the South African Beaufort Group has provided precise age constraints for several volcanic ash beds intercalated with Permian biozones within the Main Karoo Basin, from which the top of the *Tapinocephalus* AZ was determined to be older than 261.241 ± 0.088 Ma [27]. This was based on a date considered to be within the lower part of the overlying *Pristerognathus*

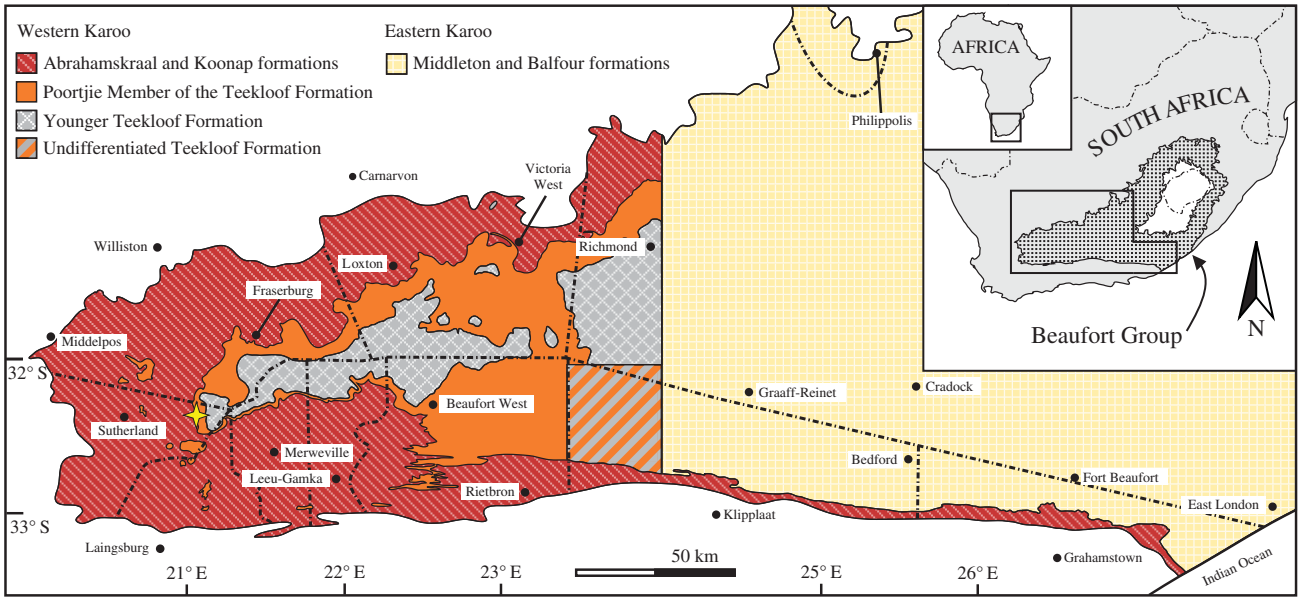

Figure 2. Map of the lowest Beaufort Group in the South African Karoo Basin. Star, locality of tuff sample (K1202-B1) on the farm Puntkraal, Sutherland district, Northern Cape Province. Alternating long and short dashed lines, boundaries of the sectors used when calculating the stratigraphic position of fossil specimens. The Philippolis sector is isolated as no fossil material has been found in the lowest Beaufort strata between the eastern limit of the Victoria West sector and the vicinity of Philippolis. (Online version in colour.)

AZ; however, the dated horizons are located in the southeast of the Karoo Basin, where few fossil specimens have been recorded from these biozones and thus biostratigraphic resolution is correspondingly poor. The precise age of the dinocephalian extinction event therefore remains poorly constrained.

2. Material and methods

(a) Genus stratigraphic ranges

The stratigraphic ranges of 54 tetrapod genera, represented by 1953 specimens from the Abrahamskraal Formation and overlying Poortjie Member of the Teekloof Formation, were recalculated from the stratigraphic positions of all known genus occurrences within the Karoo Basin. Generic occurrences were taken initially from the Beaufort Fossil Vertebrate GIS database, maintained by the Evolutionary Studies Institute (ESI) in Johannesburg, which records locality data for 13 596 fossil specimens curated in South Africa that are identified to genus level. The GIS data were imported into .kmz format and thereafter into Google Earth from where the surface geology could be seen. To this were added 37 specimens from foreign or other collections and 103 specimens collected during ongoing fieldwork by the ESI (see the electronic supplementary material, Methods). All 1953 fossil specimens used in this study are listed in the electronic supplementary material, table S1.

The Karoo Basin (approx. 600 000 km^2) was split into 10 sectors to account for lateral variation in stratigraphy (figure 2), within which fossil specimens occurring in the Abrahamskraal Formation and the Poortjie Member of the Teekloof Formation were given stratigraphic positions using 50 m stratigraphic bins for the Abrahamskraal Formation and Lower, Middle and Upper divisions for the Poortjie Member (see the electronic supplementary material, Methods and table S1). This enabled the range of each genus to be calculated within each sector, which was subsequently used in the constrained optimization (CONOP) analysis (see the electronic supplementary material, table S2). A composite section showing tetrapod-stratigraphic ranges throughout the basin was compiled using correlation of the Abrahamskraal–Teekloof Formation contact.

(b) Constrained optimization (CONOP)

Owing to the uneven recovery of fossils across the Karoo Basin, the 10 sectors differ in detail concerning the sequence of genus appearances and disappearances. The best record combines information from all sectors (see the electronic supplementary material, table S2). When sections are combined by lithological correlation, using presence or absence values within stratigraphic bins, genus range-ends are grouped at equivalent intervals. Such grouping tends to inflate generic richness, so to mitigate this we also sought fully resolved composite sequences of first and last appearances using CONOP. The resulting composite sequences achieve best-fit event ordering in relation to all the locally preserved sequences and do not rely upon lithostratigraphic boundaries for correlation between sectors. Best-fit was found by minimizing the net adjustments required to make the sequence in every sector match a single sequence. Adjustments were limited to range extension and subject to the constraint that any viable sequence must reproduce all observed coexistences of genera. Sequences were optimized, from a random starting sequence, using the simulated annealing heuristic as implemented by the CONOP algorithms [28]. After an optimal sequence was reached, the spacing between events was scaled using the mean thickness between adjacent events in the local sectors.

The optimization does not use the local positions of lithostratigraphic boundaries. To provide a link between this arbitrary scale and the lithostratigraphy, lithostratigraphic boundaries were entered as separate events in each section. Thus, they are not forced to be correlative, but find their position in the composite according to the local taxon ranges. The algorithm was constrained to maintain only the known superpositional order of the formations. This was achieved by adding a stratigraphic 'pseudo-section' that included only the lithostratigraphic boundaries—one event level for each boundary. The optimized composite sequences then emerged with a suite of local events for each boundary that did not overlap with events for other boundaries and could be attached as conservative estimates to the arbitrary scale (figure 3).

Because the CONOP analysis requires knowledge of first and last appearances, genera whose minimum stratigraphic ranges in any one sector were poorly constrained were excluded from the analysis. Genera with uncertain taxonomic validity were also

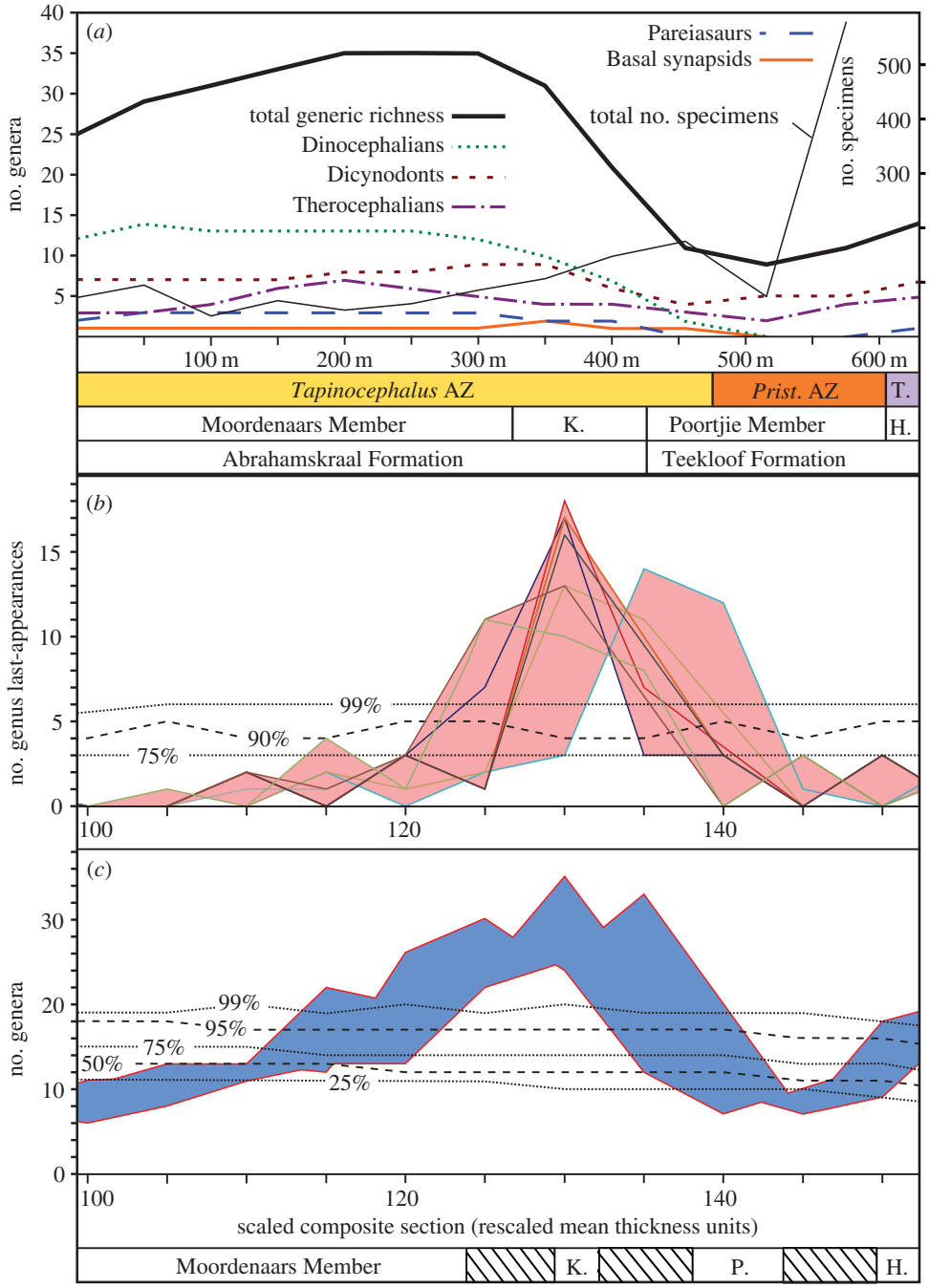

Figure 3. Generic richness and generic last-appearance events. (*a*) Raw generic richness data for composite stratigraphic section. H, Hoedemaker Member; K, Karelskraal Member; P, Poortjie Member; T, *Tropidostoma* AZ. (*b*) Uncertainty band (shaded) for best-fit composite sequences of last-appearance events per five composite sequence units (solid lines). Dashed lines, percentile outcomes for 300 random reordering events using the same genus durations. (*c*) Uncertainty band for total generic richness within the upper Abrahamskraal Formation and lower Teekloof Formation. The position of lithostratigraphic boundaries can be constrained to uncertainty bands (hatched boxes on *x*-axis). (Online version in colour.)

excluded (see the electronic supplementary material, Methods and table S2).

(c) U–Pb geochronology

Zircons were separated from a white tuff layer (sample K1202-B1) 3.5 m above the basal sandstone bed of the Poortjie Member of the Teekloof Formation in the Sutherland district of the Northern Cape Province (electronic supplementary material, figure S1). Six single zircons were selected based on grain morphology using a binocular microscope and analysed by the U–Pb isotope dilution thermal-ionization mass spectrometry (ID-TIMS) technique following the detailed procedures described in Ramezani *et al*. [29] and used in Rubidge *et al*. [27]. All zircons were pre-treated by a chemical abrasion (CA-TIMS) method modified after Mattinson [30] to mitigate the effects of radiation-induced Pb loss, and spiked with the EARTHTIME ET535 mixed ^{205}Pb–^{233}U–^{235}U tracer prior to dissolution and analysis. Uranium and lead isotopic data reduction, date calculation and propagation of uncertainties were carried out using computer applications and algorithms of Bowring *et al*. [31] and McLean *et al*. [32]. Complete U–Pb data appear in the electronic supplementary material, figure S1 and table S3.

A sample date is calculated based on the weighted mean $^{206}Pb/^{238}U$ date of a statistically coherent cluster of the youngest zircon analyses consisting of three or more data points, which is interpreted as the age of pyroclastic eruption and a maximum estimate of the depositional age of the tuff. Uncertainties are reported at 95% confidence level and follow the notation $\pm X/Y/Z$ Ma, where X is the internal (analytical) uncertainty in the

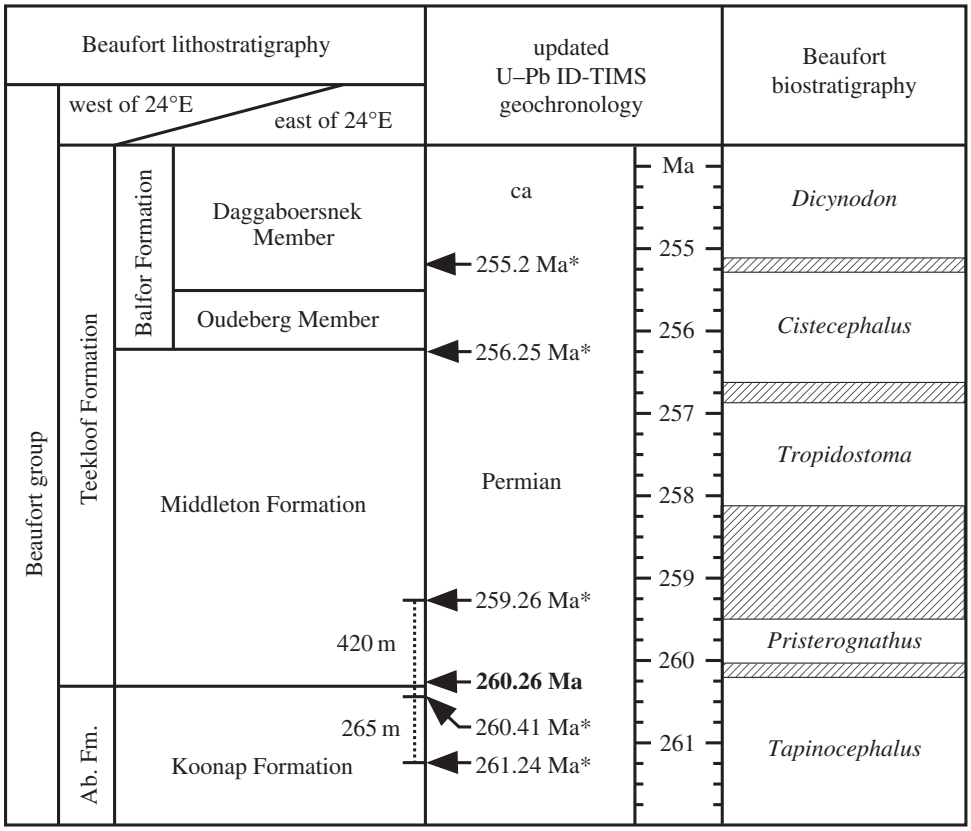

Figure 4. Recalibrated ages for Permian Beaufort Group biozones. Dated horizons are shown in lithostratigraphic position. Hashed boxes, uncertainty surrounding stratigraphic position of assemblage zone boundaries relative to dated horizons. New date in bold. All units are scaled to time. Asterisk, date obtained from [27].

absence of all external errors, *Y* incorporates the U–Pb tracer calibration error and *Z* includes the latter as well as the decay constant errors of Jaffey *et al*. [33]. Complete uncertainties (*Z*) are necessary for comparison between age data from different isotopic chronometers (e.g. U–Pb versus $^{40}Ar/^{39}Ar$).

3. Results

(a) Taxonomic turnover

We present a comprehensive late Guadalupian tetrapod biostratigraphy based on a faunal analysis of 1915 specimens, belonging to 52 tetrapod genera (excluding gorgonopsians and temnospondyls) recovered from the lower Beaufort Group throughout the main Karoo Basin. Extensive fieldwork and map-based labwork allowed fossil specimens to be assigned to one or more 50 m stratigraphic bins within the upper Abrahamskraal Formation and lower Teekloof Formation of the Karoo Basin. Raw richness counts within stratigraphic bins suggest a decline from 35 genera to 10 from the Moordenaars Member to the mid-Poortjie Member, representing approximately 71% loss of generic richness (figure 3*a*).

Because preserved ranges underestimate true ranges [34], the severity of extinction can be independently and more finely resolved using CONOP. Several equally good solutions all reveal a significant clustering of last appearances, which supports the existence of coordinated extinctions and indicates that genus richness was lost as a result of an increased extinction rate, not merely a drop in originations (figure 3*b*). In the majority of best-fit sequences recovered by CONOP there is a peak in last appearances within the Karelskraal Member of the uppermost Abrahamskraal Formation (figure 3*b*). Instantaneous generic richness may have peaked between 29 and 35, before falling to between 7 and 8, thus suggesting a statistically significant 74–80% loss of generic richness between the Karelskraal Member and the middle Poortjie Member (figure 3*c*). These data suggest that immediately preceding the peak in last-appearance events per-taxon extinction counts were approximately 0.15, rising more than threefold to approximately 0.5 at the peak before declining to approximately 0.2 after generic richness reached its minimum.

(b) Age of the *Tapinocephalus–Pristerognathus* AZ boundary

Here we report a new U–Pb zircon date (CA-TIMS method) of $260.259 \pm 0.081/0.14/0.31$ Ma based on the weighted mean $^{206}Pb/^{238}U$ date of four overlapping zircon analyses from a tuff bed situated 3.5 m above the basal sandstone of the Poortjie Member of the Teekloof Formation in the western Karoo Basin (Northern Cape Province). Biostratigraphically, this is well constrained by local fossil occurrences and basin-wide fossil datasets to the uppermost *Tapinocephalus* AZ, close to the boundary with the overlying *Pristerognathus* AZ and thus provides a precise maximum age constraint on the *Tapinocephalus–Pristerognathus* AZ boundary (figures 1 and 4). This supersedes the previously reported U–Pb date of more than 261.241 ± 0.088 Ma (or older) for the same AZ boundary in the southeastern Karoo Basin [27] (see the electronic supplementary material, Discussion).

4. Discussion

Of the higher taxa, the greatest levels of extinction occur in the clade Dinocephalia, which went extinct with its 16

genera present in the pre-extinction Moordenaars Member. Secondly, all three stem-group genera of *Tapinocephalus* AZ pareiasaurian parareptiles became extinct, although more advanced, crown-group pareiasaurs had reappeared in the Karoo Basin by the Late Permian *Tropidostoma* AZ [35,36]. The disappearance of both genera of varanopids in this interval heralded the final extinction of pelycosaur-grade synapsids. Among dicynodonts and therocephalians, no supra-generic losses occurred within the extinction interval and the decrease in generic richness was only moderate. The end-*Tapinocephalus* AZ extinction was therefore characterized by a decrease in generic richness across all major taxa, although perhaps nearly half of this resulted from the elimination of the species-rich dinocephalian clade. Conversely, the extinction of the less diverse basal pareiasaurs and varanopid synapsids had less impact of overall generic diversity. The fact that the dinocephalians and basal pareiasaurs were the largest animals in the *Tapinocephalus* AZ alludes to selectivity against ecological traits associated with large body size.

Combined with a U–Pb CA-TIMS maximum age constraint of 255.2 ± 0.16 Ma for the top of the *Cistecephalus* AZ [27], our new date of 260.259 ± 0.081 Ma from the uppermost *Tapinocephalus* AZ suggests the combined duration of the *Pristerognathus*, *Tropidostoma* and *Cistecephalus* AZs would have been approximately 5 Myr (figure 4). This contrasts with an estimated duration of 3 Myr for the overlying *Dicynodon* AZ alone [27]. The duration of the *Tapinocephalus* AZ is more difficult to estimate as although U–Pb zircon ages (*in situ* secondary ion mass spectrometry) ranging from 264 to 268 Ma have been obtained from the lower Abrahamskraal Formation [24], these have uncertainties on the order of 2–6 Myr and are not biostratigraphically well constrained. The biochronology of the Permian Beaufort Group would therefore benefit most from more precise age constraints on the *Eodicynodon* AZ and the very lowest Beaufort Group strata.

Our U–Pb date of 260.259 ± 0.081 Ma for the uppermost *Tapinocephalus* AZ constrains the end-*Tapinocephalus* AZ extinctions to the Late Capitanian [37]. This age is predicated upon the age of the GLB being isochronous with or shortly postdating the uppermost felsic ignimbrites of the central Emeishan LIP, for which an age of 259.1 ± 0.5 Ma has recently been retrieved [12]. Combined with additional U–Pb CA-TIMS ages from intrusive rocks of the Emeishan LIP, this age indicates rapid emplacement between *ca* 260 Ma and 259.1 ± 0.5 Ma [11,12] and suggests that the end-*Tapinocephalus* AZ extinctions may have coincided with the initial stages of volcanism within the Emeishan LIP, as has been done for the extinctions of at least some marine organisms [7,8].

The presumed close temporal relationship between the marine and plant extinctions and the Emeishan LIP has prompted much debate surrounding a link between the two (e.g. [7,11,13,38–40]). The new age of approximately 260 Ma for the top of the *Tapinocephalus* AZ in South Africa is consistent with a further temporal link between Emeishan volcanism and tetrapod extinctions. If this was the case then it would circumstantially implicate Emeishan volcanism as a causal factor. The existence of a concurrent tetrapod extinction event in the non-marine Karoo Basin, situated thousands of kilometres from the Emeishan LIP, would also suggest an extinction mechanism with a global influence, such as atmospheric disruption through the release of volcanic gases and large-scale contact metamorphism of biogenic rocks [11,39,41,42]. New geochemical data from the GLB at geographically disparate localities is not consistent with global warming resulting from the large-scale release of methane or volcanic CO_2 [20] and stable or cooling conditions may in fact have prevailed [43]. Acidification, short-term cooling and volcanically induced darkness, possibly linked to the onset of Emeishan volcanism, appear to be the most probable causes of extinction for marine animals at the end of the Guadalupian [39] and this could have affected terrestrial ecosystems through reduced photosynthesis. While it is tempting to conclude the existence of concurrent marine and terrestrial extinction events driven by LIP volcanism, proving concurrence is extremely difficult as the duration and timing of the Emeishan LIP and the age of the GLB are at present insufficiently constrained. The mechanisms driving elevated extinction rates among mid-Permian tetrapods are also poorly understood and there is as yet no robust geochemical evidence to support an increased volcanic influence in the Karoo.

5. Conclusion

Although not as catastrophic as that at the end of the Permian, the mid-Permian extinction on land was a significant event in which the tetrapod fauna experienced a 74–80% loss of generic richness. This was mostly because of the extinction of all dinocephalian therapsids and, although many basal genera disappeared and all major tetrapod taxa suffered some loss of generic richness, overall higher taxon extinctions were not severe. The ecological gap left by the loss of the diverse large-bodied elements of the fauna and the widespread reduction in generic richness probably became governing factors in the appearance of large gorgonopsians and dicynodonts and of small therocephalians in the late Permian *Tropidostoma* and *Cistecephalus* AZs [35].

The date (approx. 260 Ma) for the base of the Poortjie Member of the Abrahamskraal Formation provides a high-precision maximum age constraint on the *Tapinocephalus*–*Pristerognathus* AZ boundary in the Main Karoo Basin and indicates that the mid-Permian extinction event occurred close to the end of the Capitanian. This is later than the most recent estimates have suggested. Temporal constraints on Emeishan volcanism and the marine as well as the floral extinctions must be tightened before the existence of a global intra-Capitanian extinction can be properly assessed, but the new late Capitanian age for the terrestrial extinction event does support the possibility that all phenomena occurred within the same estimated time frame.

Data accessibility. The datasets supporting this article have been uploaded as part of the electronic supplementary material.

Authors' contributions. B.R. conceived the initial idea for the study and provided data on the stratigraphic position of fossil material in existing collections. M.D., B.R. and F.A. conducted the fieldwork. M.D. compiled fossil data. S.B. and J.R. are responsible for the U–Pb CA-TIMS analyses. P.S. conducted the CONOP analyses. All authors wrote the final manuscript and aided in the interpretation of the results.

Competing interests. We declare we have no competing interests.

Funding. This work was made possible by financial support to M.D., B.R. and F.A. from the Palaeontological Scientific Trust (PAST) and its Scatterlings of Africa programmes, as well as the National Research Foundation (NRF). The support of the DST/NRF Centre of Excellence in Palaeosciences (CoE in Palaeosciences) towards this research is hereby acknowledged. The geochronology was supported by NASA Astrobiology funding to D.E. and S.B.

Acknowledgements. We wish to thank Ken Angielczyk and Jörg Fröbisch for discussions concerning dicynodonts, Ellen de Kock at the Council for Geoscience and Sheena Kaal at the Iziko South African Museum for responding promptly to many requests for specimen information, and Charlton Dube and Sifelani Jirah for conscientious preparation of fossil specimens. We are grateful to Spencer Lucas and two anonymous reviewers for valuable comments on the original manuscript.

References

1. Jin YG. 1993 The pre-Lopingian benthos crisis. *C. R. XII ICCP Buenos Aires* **2**, 269–278.
2. Stanley SM, Yang X. 1994 A double mass extinction at the end of the Paleozoic era. *Science* **266**, 1340–1344. (doi:10.1126/science.266.5189.1340)
3. Sepkoski Jr JJ. 1996 Patterns of Phanerozoic extinction: a perspective from global databases. In *Global events and event stratigraphy in the Phanerozoic* (ed. OH Walliser), pp. 35–51. Berlin, Germany: Springer.
4. Wang XD, Sugiyama T. 2000 Diversity and extinction patterns of Permian coral faunas of China. *Lethaia* **33**, 285–294. (doi:10.1080/002411600750053853)
5. Ota A, Isozaki Y. 2006 Fusuline biotic turnover across the Guadalupian-Lopingian (Middle-Upper Permian) boundary in mid-oceanic carbonate buildups: biostratigraphy of accreted limestone in Japan. *J. Asian Earth Sci.* **26**, 353–368. (doi:10.1016/j.jseaes.2005.04.001)
6. Shen SZ, Shi G. 2009 Latest Guadalupian brachiopods from the Guadalupian/Lopingian boundary GSSP section at Penglaitan in Laibin, Guangxi, South China and implications for the timing of the pre-Lopingian crisis. *Palaeoworld* **18**, 152–161. (doi:10.1016/j.palwor.2009.04.010)
7. Wignall PB *et al*. 2009 Volcanism, mass extinction, and carbon isotope fluctuations in the Middle Permian of China. *Science* **324**, 1179–1182. (doi:10.1126/science.1171956)
8. Bond DPG, Hilton J, Wignall PB, Ali JR, Stevens LG, Sun Y, Lai X. 2010 The Middle Permian (Capitanian) mass extinction on land and in the oceans. *Earth Sci. Rev.* **102**, 100–116. (doi:10.1016/j.earscirev.2010.07.004)
9. Leonova TB. 2011 Permian ammonoids: biostratigraphic, biogeographical, and ecological analysis. *Paleontol. J.* **45**, 1206–1312. (doi:10.1134/S0031030111100029)
10. Bond DPG, Wignall PB, Joachimski MM, Sun Y, Savov I, Grasby SE, Beauchamp B, Blomeier DPG. In press. An abrupt extinction in the Middle Permian (Capitanian) of the Boreal Realm (Spitsbergen) and its link to anoxia and acidification. *Geol. Soc. Am. Bull.* **127**. (doi:10.1130/B31216.1)
11. Shellnutt JG, Denyszyn SW, Mundil R. 2012 Precise age determination of mafic and felsic intrusive rocks from the Permian Emeishan Large Igneous Province (SW China). *Gondwana Res.* **22**, 118–126. (doi:10.1016/j.gr.2011.10.009)
12. Zhong YT, He B, Mundil R, Xu YG. 2014 CA-TIMS zircon U-Pb dating of felsic ignimbrite from the Binchuan section: implications for the termination age of Emeishan Large Igneous Province. *Lithos* **204**, 14–19. (doi:10.1016/j.lithos.2014.03.005)
13. Stevens LG, Hilton J, Bond DP, Glasspool IJ, Jardine PE. 2011 Radiation and extinction patterns in Permian floras from North China as indicators for environmental and climate change. *J. Geol. Soc.* **168**, 607–619. (doi:10.1144/0016-76492010-042)
14. Rubidge BS. 2005 27th Du Toit memorial lecture: re-uniting lost continents. Fossil reptiles from the ancient Karoo and their wanderlust. *S. Afr. J. Geol.* **108**, 135–172. (doi:10.2113/108.1.135)
15. Lucas SG. 2009 Timing and magnitude of tetrapod extinctions across the Permo-Triassic boundary. *J. Asian Earth Sci.* **36**, 491–502. (doi:10.1016/j.jseaes.2008.11.016)
16. Rubidge BS. 1995 *Biostratigraphy of the Beaufort Group (Karoo Supergroup)*. South African Committee for Stratigraphy Biostratigraphic Series 1, Council for Geoscience Pretoria.
17. Boonstra LD. 1969 The fauna of the *Tapinocephalus* zone (Beaufort beds of the Karoo). *Ann. S. Afr. Mus.* **56**, 1–73.
18. King GM. 1990 Dicynodonts and the end Permian event. *Palaeontol. Afr.* **27**, 31–39.
19. Retallack GJ, Metzger CA, Greaver T, Jahren AH, Smith RMH, Sheldon ND. 2006 Middle-Late Permian mass extinction on land. *Geol. Soc. Am. Bull.* **118**, 1398–1411. (doi:10.1130/B26011.1)
20. Jost AB, Mundil R, He B, Brown ST, Altiner D, Sun Y, DePaolo DJ, Payne J. 2014 Constraining the cause of the end-Guadalupian extinction with coupled records of carbon and calcium isotopes. *Earth Planet Sci. Lett.* **396**, 201–212. (doi:10.1016/j.epsl.2014.04.014)
21. Lozovskiy V. 1992 The Permian-Triassic in Continental series of Laurasia and its correlation with the marine scale. *Int. Geol. Rev.* **34**, 1008–1014. (doi:10.1080/00206819209465650)
22. Menning M. 2000 Magnetostratigraphic results from the Middle Permian type section, Guadalupe Mountains, West Texas. *Permophiles* **37**, 16.
23. Henderson CM, Davydov VI, Wardlaw BR, Gradstein FM, Hammer O. 2012 The Permian period. In *The geologic time scale* (eds FM Gradstein, JG Ogg, MD Schmitz, GM Ogg), pp. 653–679. Amsterdam, The Netherlands: Elsevier.
24. Lanci L, Tohver E, Wilson A, Flint S. 2013 Upper Permian magnetic stratigraphy of the lower Beaufort Group, Karoo Basin. *Earth Planet Sci. Lett.* **375**, 123–134. (doi:10.1016/j.epsl.2013.05.017)
25. Golubev VK. 2005 Permian tetrapod stratigraphy. *New Mexico Mus. Nat. Hist. Sci. Bull.* **30**, 95–99.
26. Kurkin AA. 2011 Permian anomodonts: paleobiogeography and distribution of the group. *Paleontol. J.* **45**, 432–444. (doi:10.1134/S0031030111030075)
27. Rubidge BS, Erwin DH, Ramezani J, Bowring SA, de Klerk WJ. 2013 High-precision temporal calibration of Late Permian vertebrate biostratigraphy: U-Pb zircon constraints from the Karoo Supergroup, South Africa. *Geology* **41**, 363–366. (doi:10.1130/G33622.1)
28. Sadler PM. 2004 Quantitative biostratigraphy—achieving finer resolution in global correlation. *Annu. Rev. Earth Planet Sci.* **32**, 187–213. (doi:10.1146/annurev.earth.32.101802.120428)
29. Ramezani J, Hoke GD, Fastovsky DE, Bowring SA, Therrien F, Dworkin SI, Atchley SC, Nordt LC. 2011 High-precision U-Pb zircon geochronology of the Late Triassic Chinle Formation, Petrified Forest National Park (Arizona, USA): temporal constraints on the early evolution of dinosaurs. *Geol. Soc. Am. Bull.* **123**, 2142–2159. (doi:10.1130/B30433.1)
30. Mattinson JM. 2005 Zircon U/Pb chemical abrasion (CA-TIMS) method; combined annealing and multi-step partial dissolution analysis for improved precision and accuracy of zircon ages. *Chem. Geol.* **220**, 47–66. (doi:10.1016/j.chemgeo.2005.03.011)
31. Bowring JF, McLean NM, Bowring SA. 2011 Engineering cyber infrastructure for U-Pb geochronology: Tripoli and U-Pb_Redux. *Geochem. Geophy. Geosy.* **12**, Q0AA19. (doi:10.1029/2010GC003479)
32. McLean NM, Bowring JF, Bowring SA. 2011 An algorithm for U-Pb isotope dilution data reduction and uncertainty propagation. *Geochem. Geophy. Geosy.* **12**, Q0AA18. (doi:10.1029/2010GC003478)
33. Jaffey AH, Flynn KF, Glendenin LE, Bentley WC, Essling AM. 1971 Precision measurement of half-lives and specific activities of ^{235}U and ^{238}U. *Phys. Rev. C* **4**, 1889–1906. (doi:10.1103/PhysRevC.4.1889)
34. Signor PW, Lipps JH. 1982 Sampling bias, gradual extinction patterns and catastrophes in the fossil record. *Geol. Soc. Spec. Pap.* **190**, 291–296. (doi:10.1130/SPE190-p291)
35. Smith RHM, Rubidge BS, Van Der Walt MVM. 2012 Therapsid biodiversity patterns and palaeoenvironments of the Karoo Basin, South Africa. In *The forerunners of mammals* (ed. A Chinsamy-Turan), pp. 31–64. Indianapolis, IN: Indiana University Press.
36. Tsuji LA, Müller J. 2009 Assembling the history of the Parareptilia: phylogeny, diversification, and a new definition of the clade. *Fossil Rec.* **12**, 71–81. (doi:10.1002/mmng.200800011)
37. Angiolini L (ed.). 2014 Permian timescale. *Permophiles* **59**, 38.
38. Courtillot V, Jaupart C, Manighetti I, Tapponnier P, Besse J. 1999 On causal links between flood basalts and continental breakup. *Earth Planet Sci. Lett.* **166**, 177–195. (doi:10.1016/S0012-821X(98)00282-9)

39. Bond DPG, Wignall PB. 2014 Large igneous provinces and mass extinctions: an update. *Geol. Soc. Spec. Pap.* **505**, 29–55. (doi:10.1130/2014.2505(02))
40. Shellnutt JG. 2014 The Emeishan Large Igneous Province: a synthesis. *Geosci. Front.* **5**, 369–394. (doi:10.1016/j.gsf.2013.07.003)
41. Ganino C, Arndt NT. 2009 Climate changes caused by degassing of sediments during the emplacement of large igneous provinces. *Geology* **37**, 323–326. (doi:10.1130/G25325A.1)
42. Retallack GJ, Jahren AH. 2008 Methane release from igneous intrusion of coal during Late Permian extinction events. *J. Geol.* **116**, 1–20. (doi:10.1086/524120)
43. Sheldon ND, Chakrabarti R, Retallack GJ, Smith RMH. 2014 Contrasting geochemical signatures on land from the Middle and Late Permian extinction events. *Sedimentology* **61**, 1812–1829. (doi:10.1111/sed.12117)